Horizon 2020 - Marie Sklodowska-Curie Actions
Innovative Training Network (ITN)
Complex **Rh**Eologies in **E**arth dynamics and industrial **P**rocesses

Probing the characteristics of mush-magma transition: insights from laboratory experiments

Nicolò Sgreva Rubens

A.Davaille (FAST, Fr)
I.Kumagai (Meisei University, Japan)
K.Kurita (ERI, Japan)

Context:

Many geological dynamical processes take place in systems that are heterogeneous in composition, density and mechanical properties:

- settling of crystals and nodules in a magma chamber
- upwelling of magma bodies in heterogeneous lithosphere
- filling of fractures, etc.
- magma-mush transition

However, description and prediction of these kind of processes often require the definition of an “**effective rheology**” of the medium.

Examples

1

Dikes with country rock fragments.
Barberton Greenstone Belt, South Africa

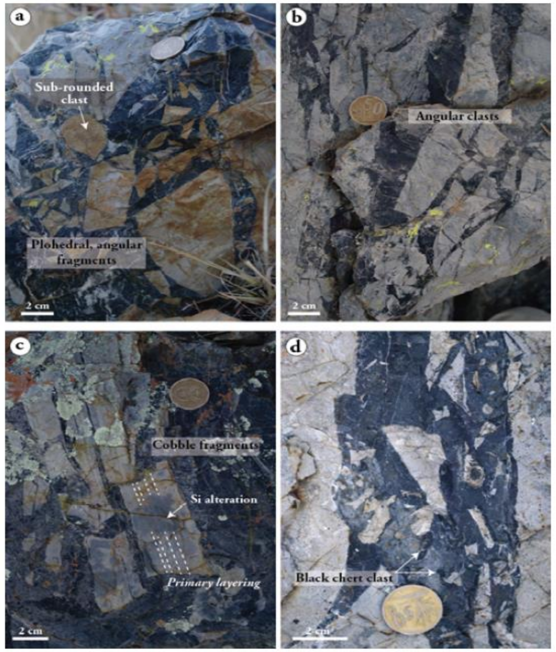

From Ledevin et al. (2015)

2

Back scattered electron images of deformed **crystal-bearing magma.**

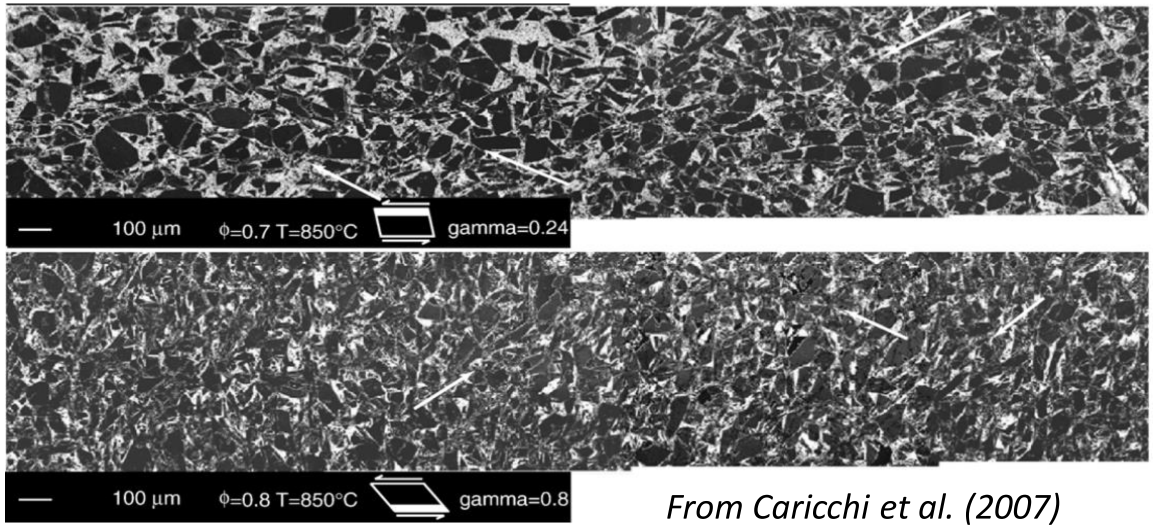

From Caricchi et al. (2007)

3

Magma – mush rheological transition:

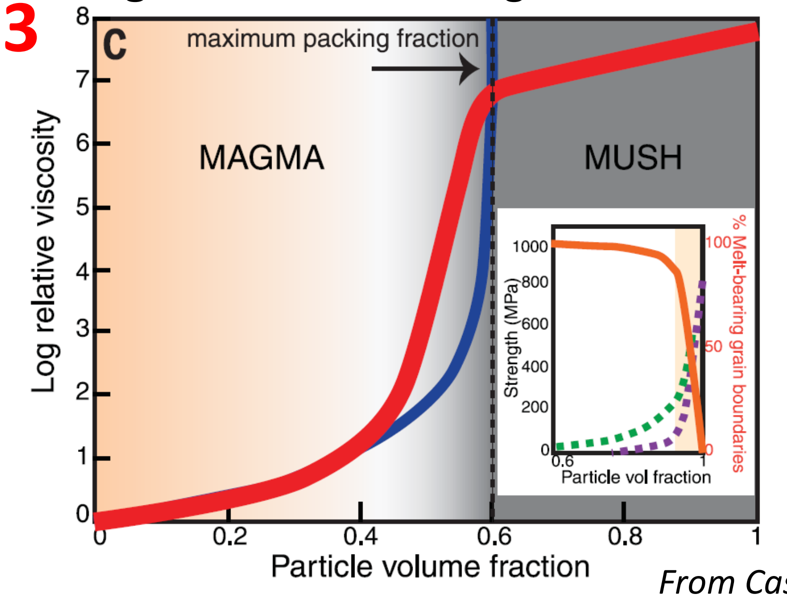

From Cashman et al. (2017)

Characteristics of those systems:

- High solid fraction ➞ **Jamming =** The local deviatoric stress has to exceed the yield stress (σ_Y) for the material to flow
- Viscosity decreases with increasing shear rate (due to increased organization) ➞ **Shear-thinning**

⬇

Effective rheology

The experiment: object falling in a fluid

- In **Newtonian** fluid, it's a classical problem and it can be used to measure the viscosity of the fluid.

If $Re \ll 1$, Terminal velocity: $v_{stokes} = \frac{2r^2 g\Delta\rho}{9\eta}$

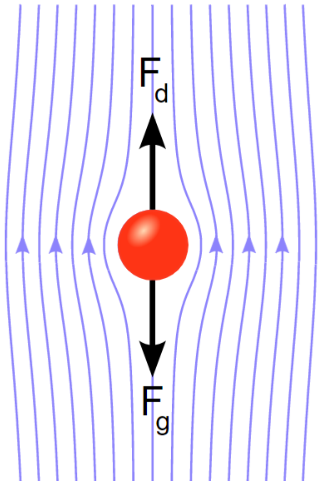

- In a **viscoplastic** fluid:
  - The yield stress (σ_Y) has to be overcome to unjam the **structure**
  - σ_Y + Shear-thinning + … ⟶ results in a complex rheology

Back scattered electron images of deformed crystal-bearing magma.

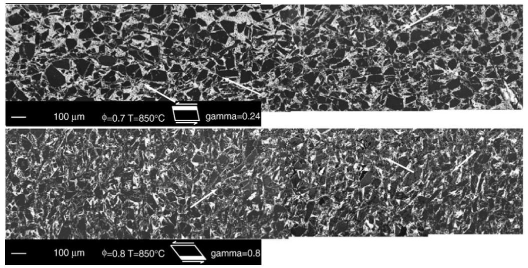

From Caricchi et al. (2007)

Carbopol

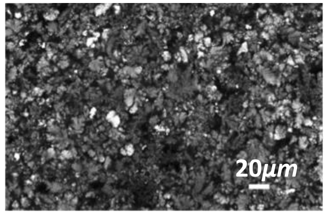

(from Gutowski et al., 2012.)

- Two end-members:

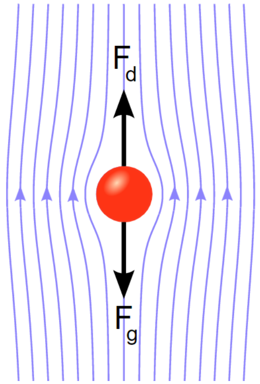

$$Size_{intruder} \ll Size_{fluid-structure}$$

Porous media

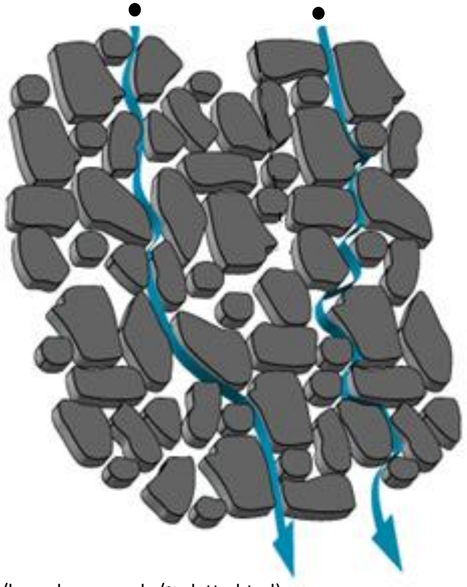

(From http://hercules.gcsuedu/~sdatta.html)

$$Size_{intruder} \simeq Size_{fluid-structure}$$

?

$$Size_{intruder} \gg Size_{fluid-structure}$$

Macroscopic flow

E.g. Carbopol

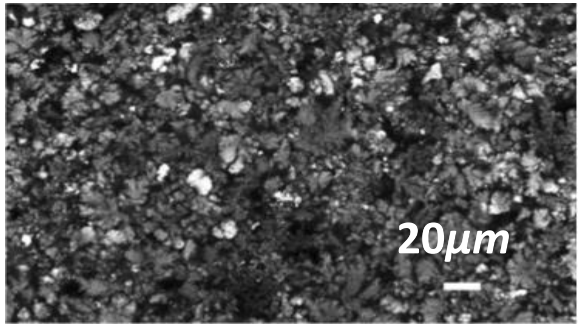

(from Gutowski et al., 2012.)

The fluid under scrutiny

- The gel is a superabsorbent polymer (**SAP**). It is polyacrylamide, made by copolymerization of acrylic acid and acrylamide

- In water, these polymer powder grains swell up to 200 times (1g of this SAP can absorb up to 200g of water) and form gel grains whose size (d_g) can be controlled by controlling the size of the initial powder.

Dry gel →

After water absorption →


Lejcuś et al. (2015)

We performed experiments with **5** different grain size gels.
The grain size distributions (by imaging analysis) and average equivalent grain sizes are:

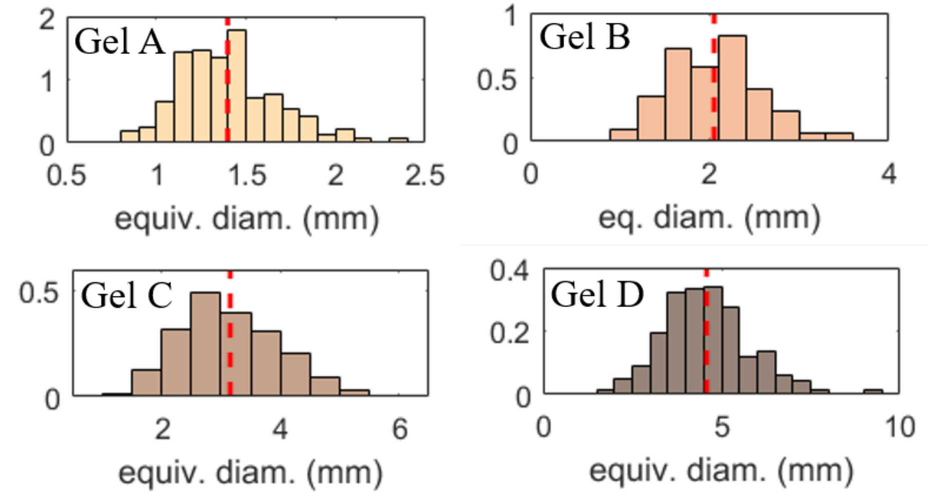

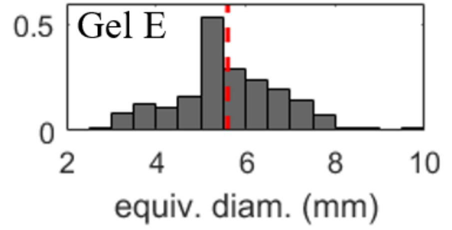

Name	Average d (mm)
Gel A	1.43
Gel B	2.11
Gel C	3.28
Gel D	4.79
Gel E	5.72

Rheological behaviour of SAPs and Carbopol gels

SAP: mixture of touching grains with a solid fraction >70%

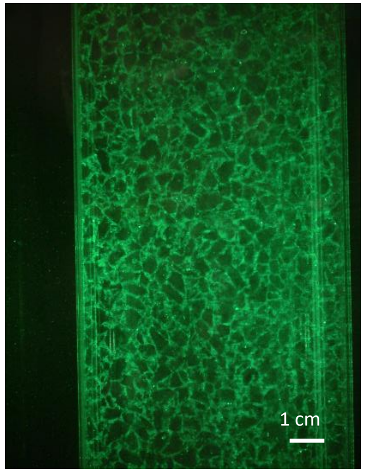

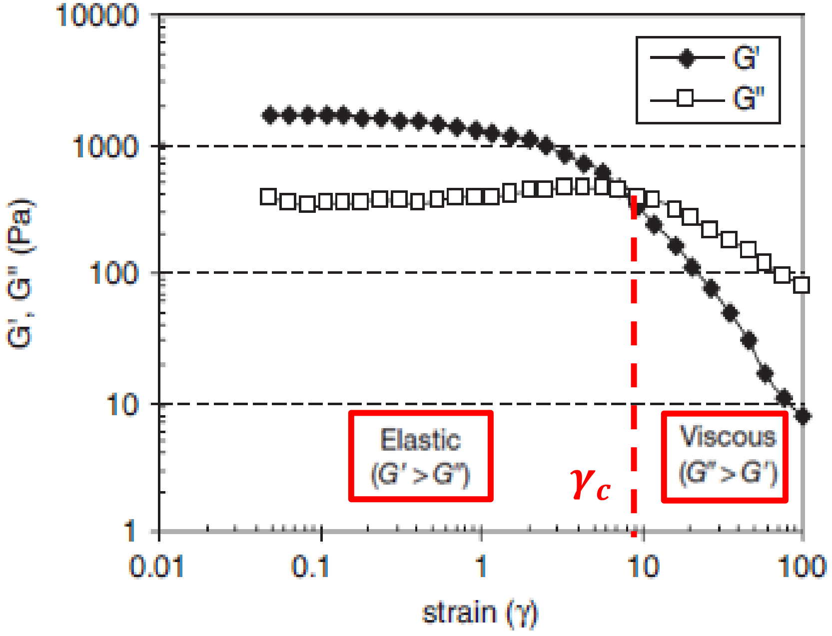

(Ramazani-Harandi et al 2006).

- Low γ: jammed particles. The all system behaves mainly elastically
- High γ: fluid-like regime
- Yield stress $\tau_Y \approx \tau_c = G'\gamma_c$

Carbopol: concentrated suspensions of microgels

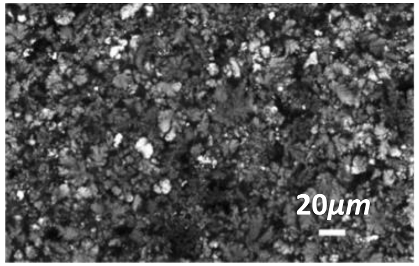

(from Gutowski et al., 2012.)

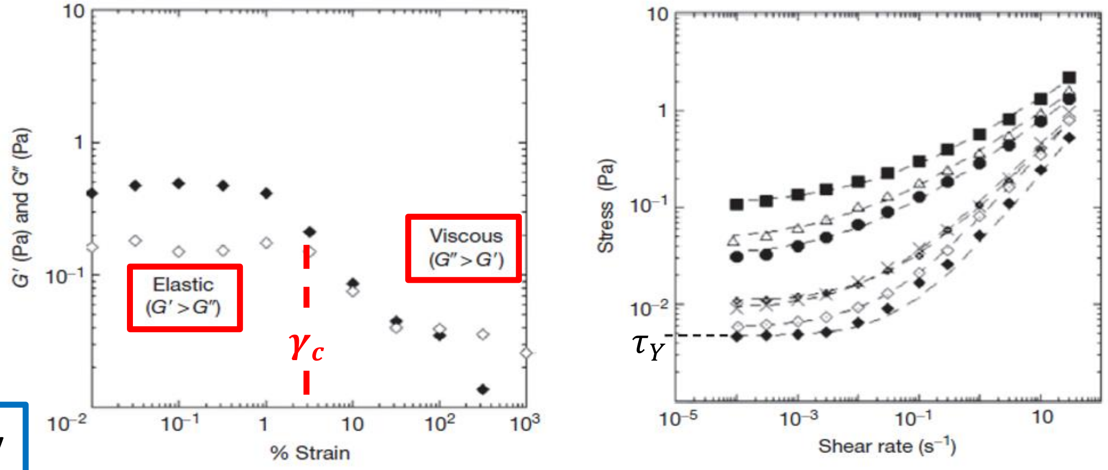

Modified from Darbouli et al (2013).

Experimental setup

- Sphere was dropped in the center of a cylindrical vessel (100 mm wide and 500 mm deep) previously filled by the gel.
- The diameter of the spheres (d_s) ranges between 3 and 30 mm. We use spheres of various materials (steel, tungsten, nickel alloy, glass) in order to cover a wide range of densities (from 2200 to 15000 kg/m^3).
- Gels have been gently stirred for 2-3 days in order to eliminate air bubbles and to avoid preferential paths between different ball releases.

Illuminated cross-section

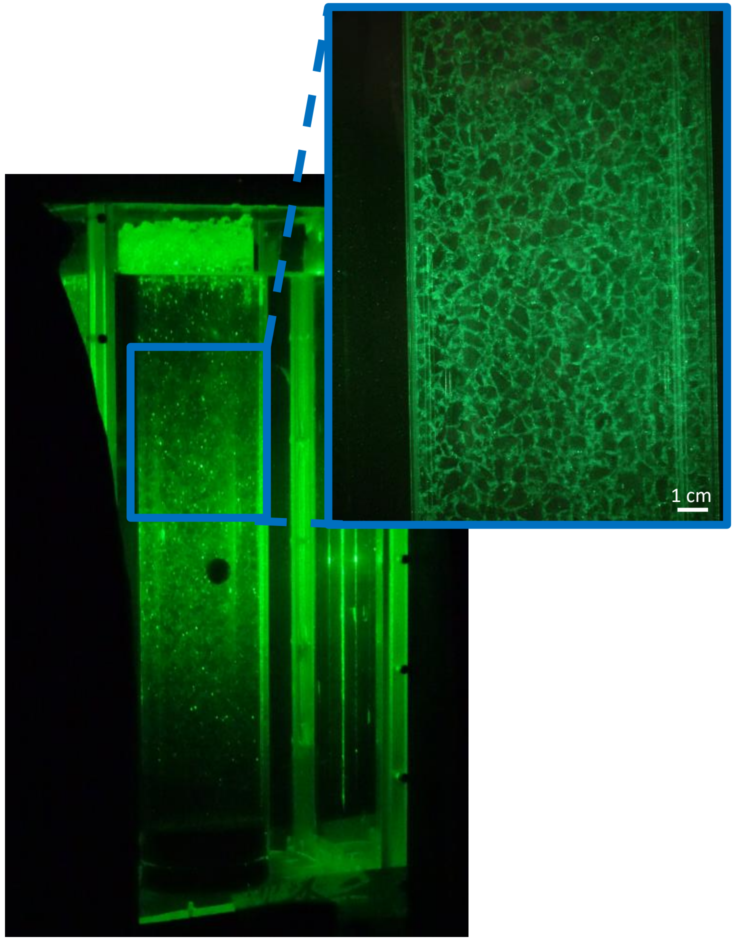

- **5 motion regimes**. For a given gel we get:

Constant ρ_s:

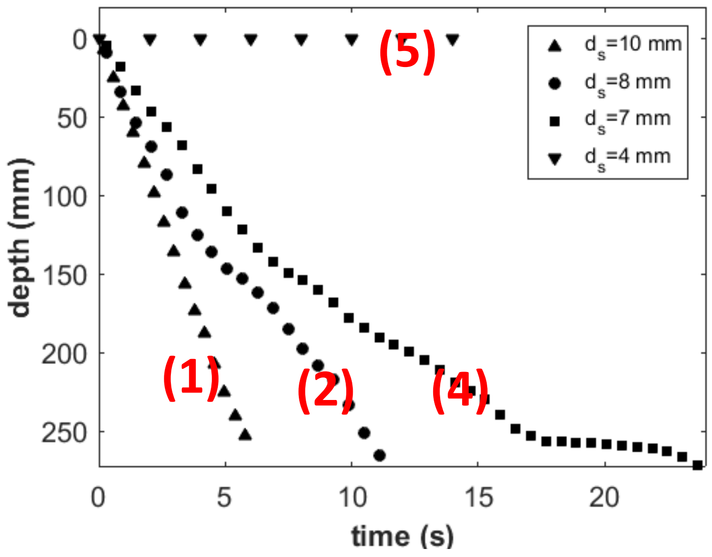

Constant d_s:

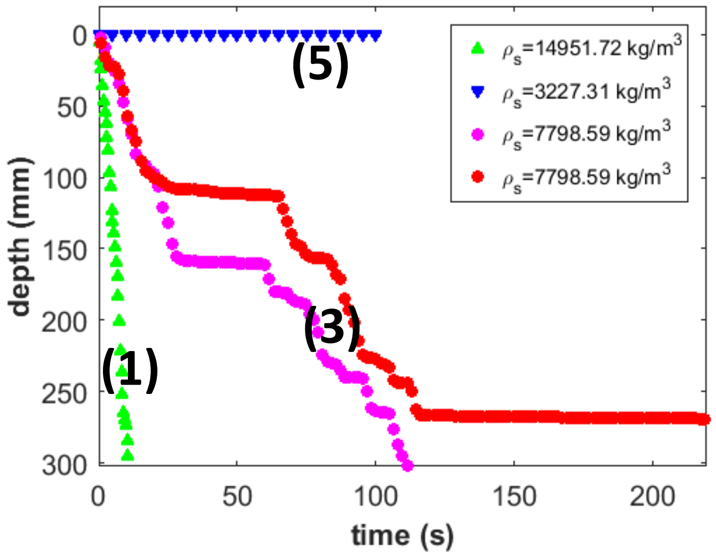

1) Linear regime: rapid and straight fall at constant terminal velocity

2) Irregular regime superimposed to linear: spheres never stop during their way down ($v_y > 0$) but their velocity varies.

3) Stop&go regime: periods of no-motion ($v_y = 0$) and periods of irregular falls follow one another

4) Logarithmic regime: a slow fall at a progressively decreasing velocity

5) No-motion

Scalings:

Taking Carbopol as end member (that is, $\boldsymbol{d_{sphere}} \gg \boldsymbol{d_{grain}}$), the slow motion of a sphere (i.e. not considering the stoppage cases) is parameterized by two key dimensionless numbers (Bingham and Yield number) and a master curve:

From Tabuteau et al (2007).

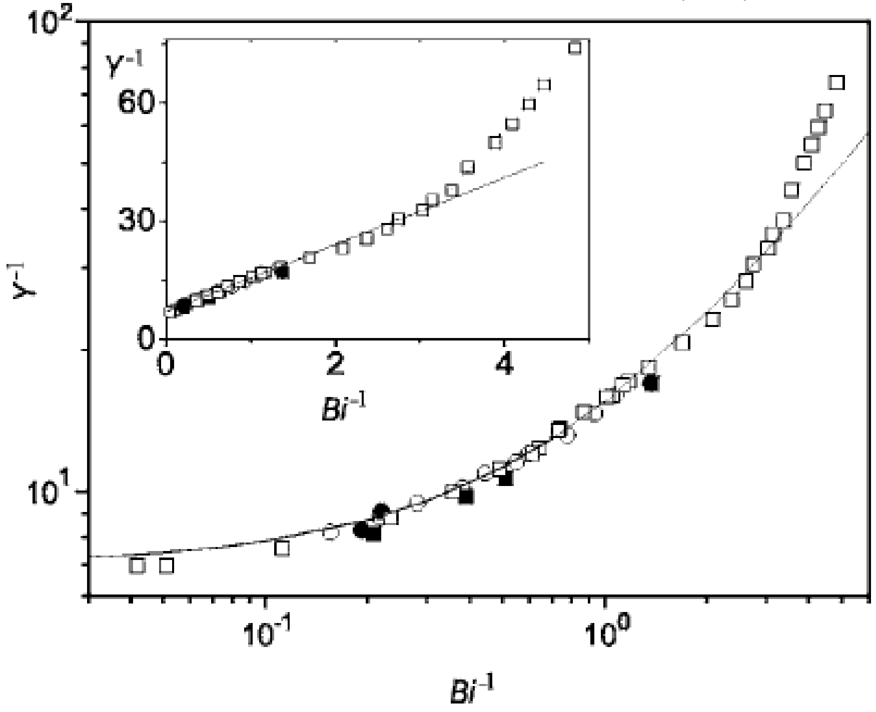

- **Two dimensionless numbers**:

The yield number: $Y = \dfrac{3\sigma_Y}{g d_s \Delta\rho}$

The Bingham number: $Bi = \dfrac{\sigma_Y}{K_v (v_y/d_s)^n}$

- **A master curve**:

$$\frac{1}{Y} = 6kX(n) + \frac{6X(n)}{Bi} = 7 + \frac{8.52}{Bi}$$

Where:

- *n = 0.5,* fitting parameter
- *k* = 0.823, found by numerical simulation (*Beaulne et al 1997*)
- *X(n) = 1.42,* drag-correction factor for power-law fluids (*Gu&Tanner.1985*)

From *Tabuteau et al. 2007*, the critical value Y_c above which there is no motion of the sphere (for $\boldsymbol{d_{sphere}} \gg \boldsymbol{d_{grain}}$) is $Y_c = 0.145$.

- Sphere-texture interaction

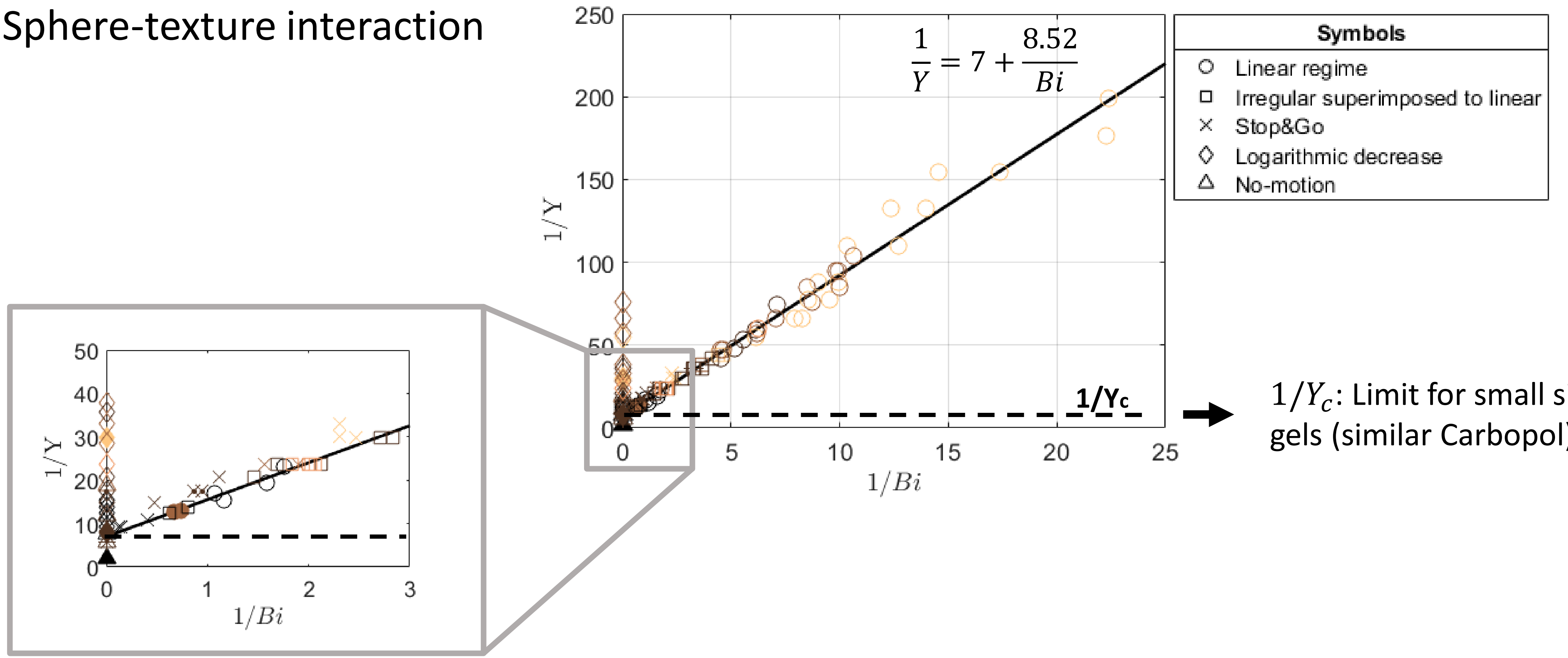

$1/Y_c$: Limit for small size gels (similar Carbopol)

In SAP, no-motion (Δ) and the logarithmic (◊) regime are also observed for $1/Y > 1/Y_c$. This is due to the interaction between spheres and the gel structure.

- Sphere-texture interaction

When $\boldsymbol{d_{sphere}} \rightarrow \boldsymbol{d_{grain}}$ the no-motion limit moves to higher $1/Y$

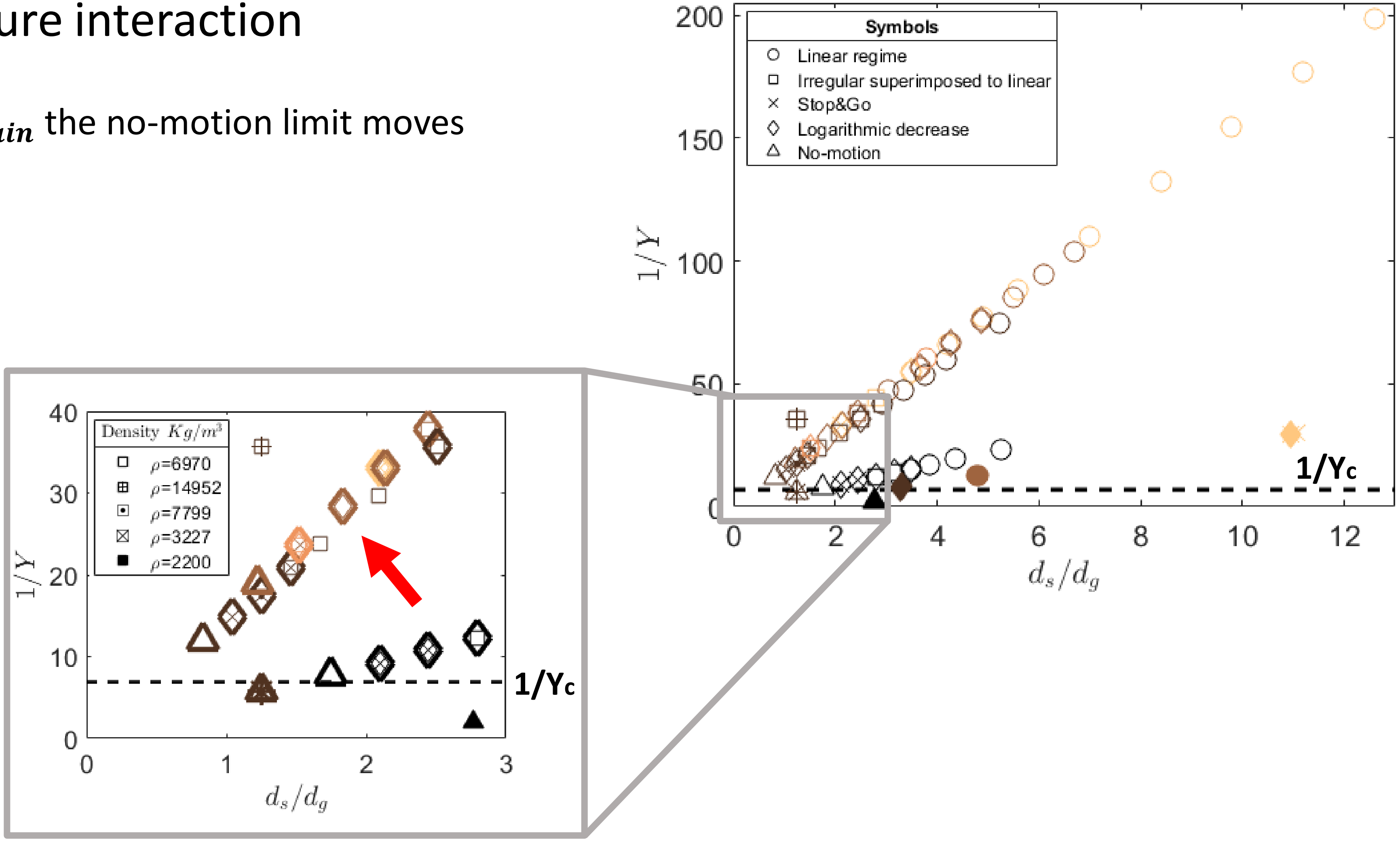

When $\boldsymbol{d_{sphere}}$ approaches $\boldsymbol{d_{grain}}$, spheres "see" obstacles on their way and the effective rheology breaks down.

- The Mush-Magma transition

Based on the observed motion regimes in our experiments, we can derive the following regime diagram for an “object” that interacts with a magmatic mush:

SAP

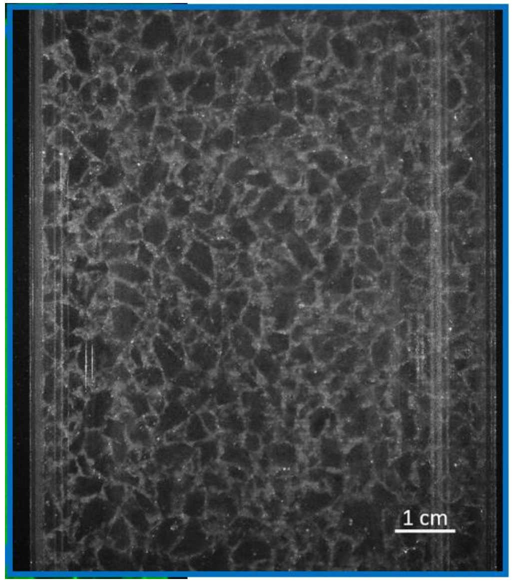

Crystal-rich magma

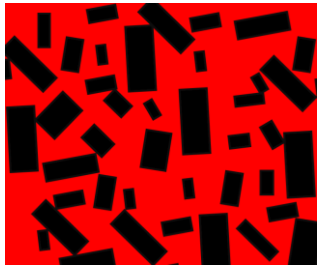

Melt-rich mush

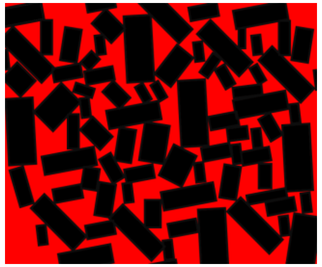

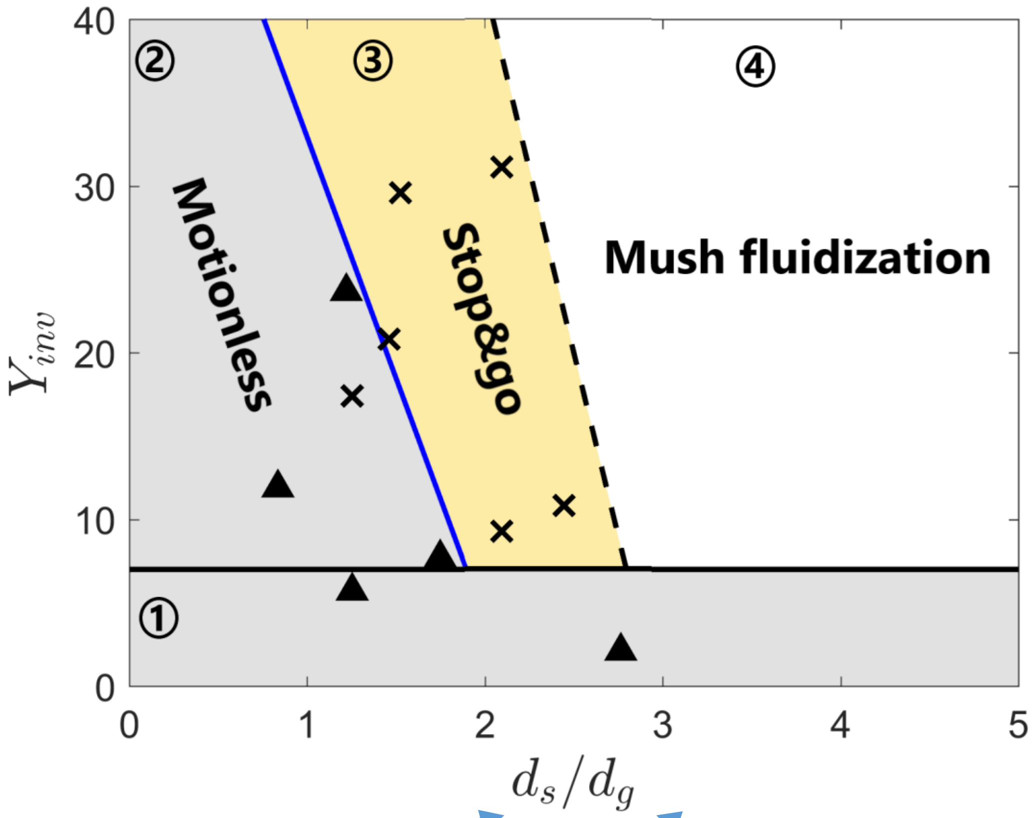

Bubble/melt pocket diameter

crystals diameter

- Motion/ no-motion conditions for a buoyant melt pocket (of diameter dI) in a crystal-rich Hershel-Bulkley magmatic reservoir:

Critical (inverse) Yield number

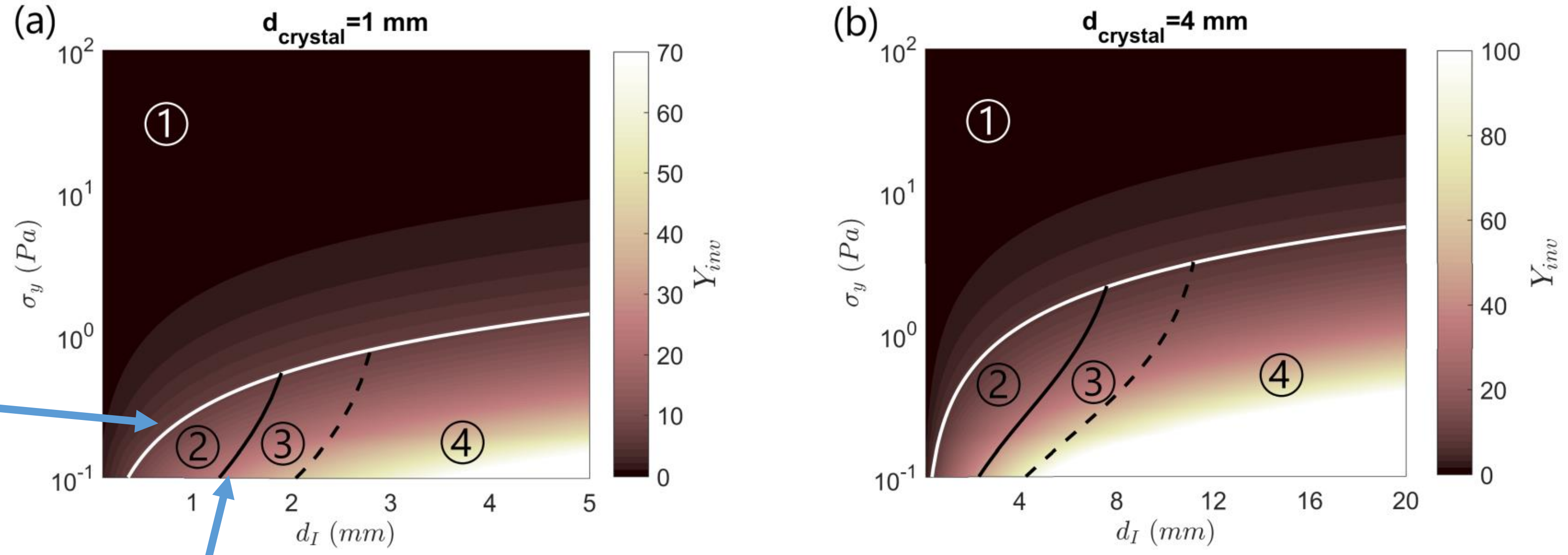

Critical (inverse) Yield number for intruder and crystals with similar size

- (1) and (2): No motion conditions
- (3): stop & go
- (4): motion conditions

- Motion/ no-motion conditions for a bubble (of diameter db) in a crystal-rich Hershel-Bulkley magmatic reservoir:

Bubbles which nucleate within a crystal mush with yield stress may or may not move through it:

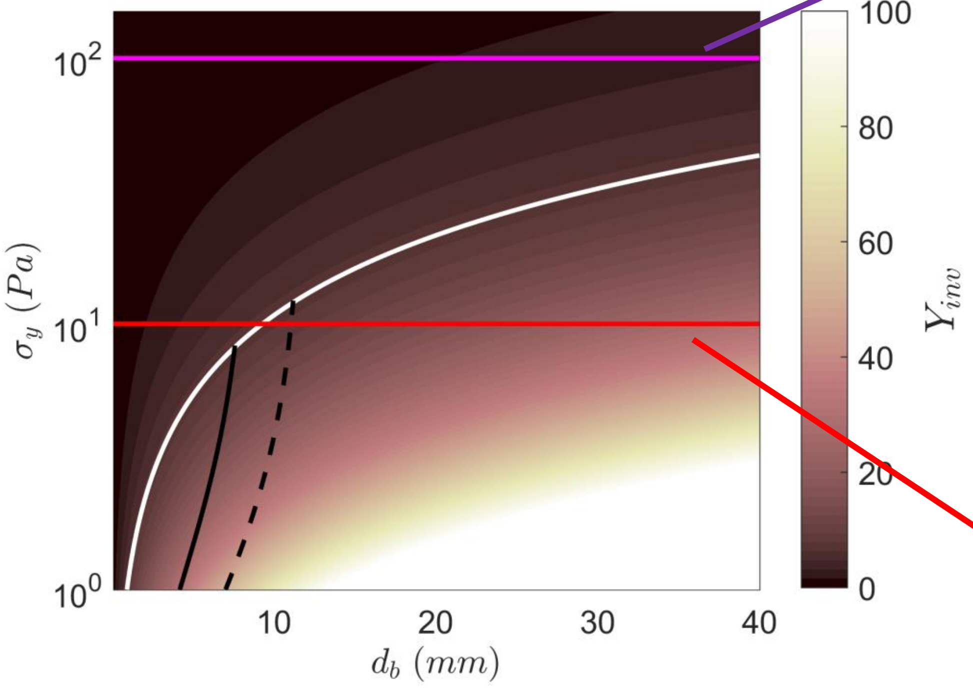

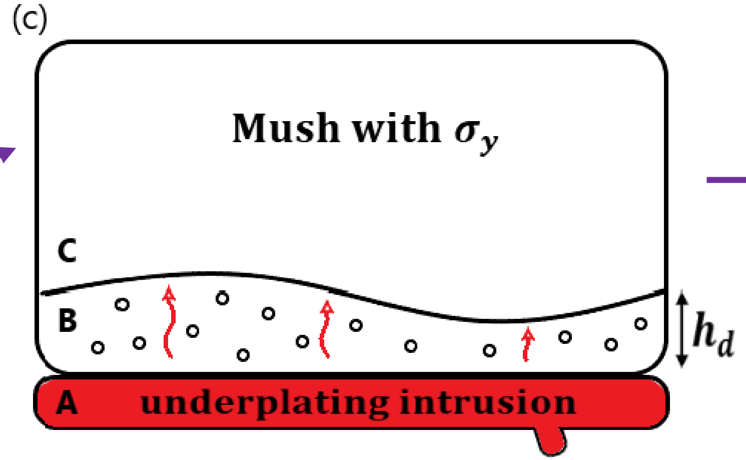

At larger yield stress, bubbles get entrapped in the mush. They can accumulate by further heating (e.g. from an intrusion)

Trigger of Rayleigh-Taylor instability?

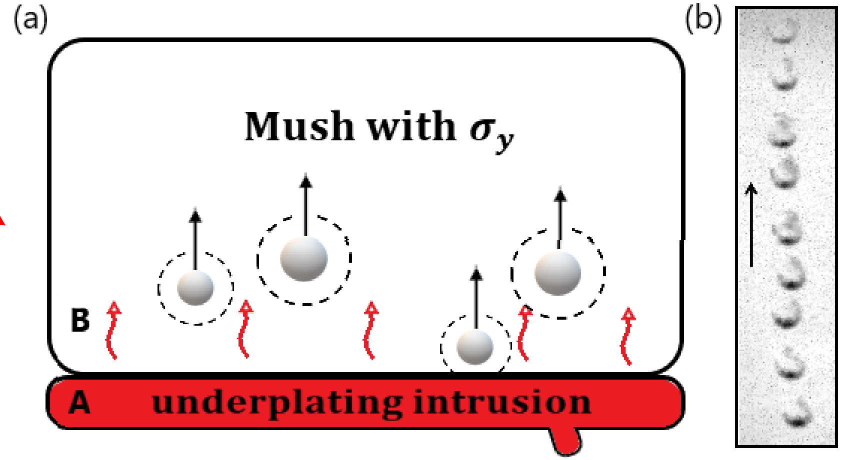

For low values of yield stress, bubbles can move upward fluidizing a region of mush around them

Conclusion

- Beside the classical steady-state motion and no-motion regimes, typical of viscoplastic fluids, the interaction between moving objects and fluid structure results in two additional regimes where motion becomes more chaotic.

- Considering the mush as a jamming material, large (and buoyant) melt intrusions or bubbles can unjam (i.e. fluidize) the mush around them and move slowly upward.

- Bubbles which nucleate in a crystal mush with yield stress may or may not move through it. In the latter case, the accumulation of entrapped bubbles can form a less dense layer. Further heating can make the layer unstable and a Rayleigh-Taylor instability might develop remobilizing the entire mush.

Literature cited

- H. Tabuteau et al., Drag force on a sphere in steady motion through a yield-stress fluid. *Journal of Rheology* 51, 125 (2007)
- I. A. Gutowski, D. Lee, J. R. de Bruyn, and B. J. Frisken. Scaling and mesostructure of carbopol dispersions. *Rheologica acta*, 51(5):441–450, 2012.
- K. V. Cashman, R. S. J. Sparks, and J. D. Blundy. Vertically extensive and unstable magmatic systems: a unified view of igneous processes. Science, 2017.
- M. Ledevin et al., The rheological behavior of fracture-filling cherts: example of Barberton Greenstone Belt, South Africa. *Solid Earth*, 6, 253-269, (2015)
- L. Caricchi et al., Non-newtonian rheology of crystal-bearing magmas and implications for magma ascent dynamics. *Earth Planet. Sci. Lett.*, 402-419, (2007)
- K. Lejcus, J. Dabrowska, D. Garlikowski, and M. Spitalniak. Innovative water absorbing geocomposite for anti-erosion protection. *Environmental Connections, Portland (OR)*, 2015.
- M. Ramazani-Harandi, M. Zohuriaan-Mehr, A. Yousefi, A. Ershad-Langroudi, and K. Kabiri. Rheological determination of the swollen gel strength of superabsorbent polymer hydrogels. *Polymer testing*, 25(4):470–474, 2006.
- M. Darbouli, C. Métivier, J.-M. Piau, A. Magnin, and A. Abdelali. Rayleigh-bénard convection for viscoplastic fluids. *Physics of Fluids*, 25(2):023101, 2013.